Monitoring Activity of the Subglacial Lake Mercer Based on CryoSat-2 and ICESat-2 Altimetry Data from 2011 to 2023

Penglan Luo [1, 2], Gang Qiao [1, 2*], Zhi Qu [1, 2], Sergey Popov [3, 4]

[1] Center for Spatial Information Science and Sustainable Development Applications, Tongji University, 1239 Siping Road, Shanghai, China - (2231985, qiaogang, 2311669)@tongji.edu.cn
[2] College of Surveying and Geo-Informatics, Tongji University, 1239 Siping Road, Shanghai, China
[3] Institute of Earth Sciences, Saint Petersburg State University, 31–33 10-ya Liniya V.O., 199178 St. Petersburg, Russia - spopov67@yandex.ru
[4] Polar Marine Geosurvey Expedition, 24 Pobedy Str., Lomonosov, 198412 St. Petersburg, Russia

Keywords: Subglacial Lakes, Satellite Altimetry, Remote Sensing, Hydrological System, Elevation Anomaly, Time Series.

Abstract

Active subglacial lakes are capable of exchanging and transporting water through water flow paths, thus having an important impact on ice sheet movement and even on the regional mass balance. The use of satellite altimetry can indirectly reveal internal subglacial hydrological activity through direct surface elevation observation, which plays an important role in the study of the evolution of active subglacial lakes. This paper monitors and analyzes the activity of the subglacial lake Mercer (SLM) in the Whillans and Mercer Ice Stream (WIS/MIS), using data from the CryoSat-2 satellite radar altimetry and ICESat-2 satellite laser altimetry. We adopt the differential DEM model and the repeat orbit model based on their respective data characteristics. Finally, we reveal the temporal and spatial evolution patterns of SLM during 2011-2023, and construct the elevation anomaly time series. The results show that the central and western parts of SLM were the areas with more significant elevation anomalies, and there were three significant fill-drain cycles during the time periods studied in this research, with the elevation anomaly range reaching about 8 m and 4 m for the first and second cycles, respectively, and the lake is currently in the third significant draining phase. Furthermore, the elevation anomalies obtained during the mission overlap time of CryoSat-2 and ICESat-2 data are in good agreement, which confirms the accuracy of our method.

1. Introduction

The widely distributed subglacial lakes are an important part of the Antarctic subglacial hydrological system. In the 1960s and 1970s, scientists detected some flat, bright, strongly reflecting echo signals on radio echo sounding (RES) data (Oswald and Robin, 1973), a phenomenon that was interpreted as the presence of subglacial water under the ice, which is the earliest and most direct proof of the existence of subglacial lakes in history. An updated global inventory published in 2022 indicates that a total of 675 subglacial lakes are currently found in Antarctica (Livingstone et al., 2022).

Unlike most of the subglacial lakes detected by RES, which are stable, i.e., not exchanging water with the outside world, some of them are "active" subglacial lakes that undergo cyclic fill-drain events that produce changes in the internal pressure of the ice sheet and lead to anomalous surface elevation changes (elevation anomalies) of the ice sheet relative to other regions. Most of the active Antarctic subglacial lakes are located at the margins of the ice sheet, and their drainage water can be transported over long distances and discharged to the ocean under the influence of hydraulic potential, thus potentially affecting the state of mass balance of the Antarctic ice sheet. Therefore, long-term monitoring of cyclic changes in the fill-drain events of active subglacial lakes is important for understanding changes in the Antarctic subglacial hydrological system and the resulting changes in the regional mass balance.

Since the beginning of this century, scientists have widely used satellite altimetry to identify and monitor changes in active subglacial lakes in Antarctica, as it can accurately obtain the surface elevation of the Antarctic ice sheet. The earliest example was the use of ERS-2 altimetry data to detect surface deformation due to a drainage event in a subglacial lake system in the region of the Adventure Trench in East Antarctica (Wingham et al., 2006). Since then, based on satellite altimetry data, scientists have carried out detailed studies on some subglacial lakes in typical areas or discovered some new subglacial lakes one after another. In Byrd Glacier, joint monitoring based on ICESat and ice velocity suggests that drainage events in subglacial lakes upstream of the Byrd Glacier have led to a rapid increase in ice velocity during the same period (Stearns et al., 2008). In the Crane Glacier of the Antarctic Peninsula, a new rapid drainage event of a subglacial lake was detected based on ICESat and airborne altimetry data (Scambos et al., 2011). In the Recovery Ice Stream region, a combination of ICESat, MODIS optical image, and RES data also identified a connected system of active subglacial lakes that can be drained in cascades over long distances (Fricker et al., 2014). In Thwaites Glacier, an active subglacial lake system was identified using CryoSat-2 data that recorded two significant drainage events in 2013 (Smith et al., 2017) and 2017 (Malczyk et al., 2020), respectively. In addition, other areas such as Cook Glacier (Miles et al., 2018; Flament et al., 2014; McMillan et al., 2013), Kamb Glacier (Kim et al., 2016), Slessor Glacier (Fan et al., 2022), and Institute Ice Stream (Siegert et al., 2014) have been monitored and analyzed by scholars using satellite altimetry data for active subglacial lake dynamics.

Satellite altimetry can be categorized into satellite radar altimetry and satellite laser altimetry according to its working principle. CryoSat-2 and ICESat-2 are the most advanced radar

* Corresponding author

altimetry and laser altimetry satellites with overlapping missions, and there have been studies of their combined use in monitoring subglacial lake activity. However, most of these studies used a single method in constructing the elevation anomaly time series and did not fully utilize the data characteristics of different altimetry data (Siegfried et al., 2023; Siegfried and Fricker, 2021). In this paper, we take one typical subglacial lake in West Antarctica as an example, combining CryoSat-2 and ICESat-2 altimetry satellite data to monitor the fill-drain events by using different data processing and calibration methods, analyzing its temporal-spatial evolution, and finally constructing the ice surface elevation anomaly time series to reflect the overall change patterns.

2. Data and Methods

2.1 Study Area

The Whillans and Mercer Ice Stream region (WIS/MIS) is a hot spot in the field of subglacial lake research (Figure 1). A large number of subglacial lakes were identified by ICESat in the early 21st century. With the development of satellite altimetry techniques, scientists analyzed the elevation changes over these areas in long-term series or by combing different altimetry missions (Siegfried and Fricker, 2021; Siegfried et al., 2014; Fricker et al., 2007). In addition to the application of satellite altimetry, ice radar (Christianson et al., 2012), seismic surveys (Horgan et al., 2012), field drilling (for SLM Lake and SLW Lake (Priscu et al., 2021; Tulaczyk et al., 2014)), and modelling (Carter et al., 2013, 2017) have been widely used in the studies of subglacial hydrologic systems in this region. In this paper, we choose Subglacial Lake Mercer (SLM), as our research target, which was drilled in December 2018.

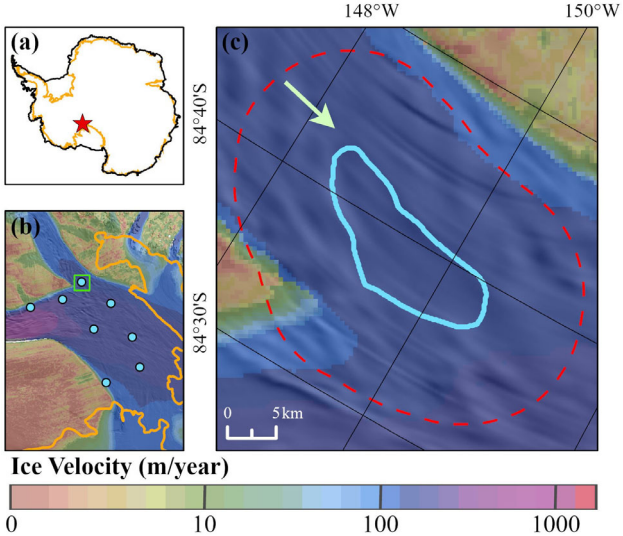

Figure 1. The location of the study area. (a) Location of the study area in Antarctica. The yellow line is the grounding line (Gardner et al., 2018). (b) Distribution of active subglacial lakes. The green rectangle indicates the locations of SLM. The blue circles are active subglacial lakes (Livingstone et al., 2022). Ice flow velocity is overlaid on the MODIS Mosaic of Antarctica (Scambos et al., 2007), as is the case in Figures 2, 4, and 6. (c) The blue line is the boundary of SLM, which is from a previous study (Siegfried and Fricker, 2018). The red dashed line is a buffer, which is 10 km from all directions of the lake. The green arrow indicates the ice flow direction.

2.2 Data

In this paper, two types of altimetry data, CryoSat-2 (2010-2021) and ICESat-2 (2018-2023), are used in combination to realize the monitoring and analysis of subglacial lake activities of SLM (Figure 2).

2.2.1 CryoSat-2 Altimetry Data: CryoSat-2 is the world's first radar altimetry satellite with an interferometric mode. CryoSat-2 operates mainly in LRM (Low Resolution Mode) and SARIn (Synthetic Aperture Radar Interferometric) modes in the Antarctic ice sheet. The LRM mode mainly works in the interior of the ice sheet, similar to ERS, Envisat, and other satellites, which is a traditional radar altimetry mode, while the SARIn mode is the most advanced mode of CryoSat-2, which mainly works at the margin of the ice sheet, whereas traditional altimetry modes have large errors due to the slope of the terrain. The SARIn mode directly determines POCA (Point of Closest Approach) from the phase information (McMillan et al., 2013) so as to obtain more accurate elevation information. The along-track resolution of SARIn mode is about 305 m, the across-track resolution is about 1.65 km, and the sample interval is about 300 m, with an accuracy of about 0.5 m on flat areas (Wang et al., 2015). We used the latest L2 baseline-E CryoSat-2's SARIn model data from January 2011 to August 2021 (the baseline-E version has been updated to August 2021 by the time of data processing in this paper), and the anomalous data were removed by combining backward scattering coefficients (> 30 dB) and data quality labels.

2.2.2 ICESat-2 Altimetry Data: ICESat-2 is the newest laser altimetry satellite, which was launched in 2018 as a follow-up mission to ICESat. The significant difference between ICESat-2 and ICESat is that ICESat-2 illuminates three pairs of six beams of 532 nm (green) lasers, which enables it to obtain finer information on ice sheet elevation changes and improve the temporal resolution of the data to a seasonal scale. ICESat-2's each pair is separated by about 3.3 km in the along-track direction, and each pair of strong and weak beam is separated by about 90 m. ICESat-2's raw sampling interval is about 0.7 m (ATL03 Global Geolocated Photon Data), and the ground footprint is about 11 m in diameter (Markus et al., 2017). Moreover, ICESat-2 operates in a continuous mode of operation, while ICESat only took about three campaigns (each lasting about 30 days) in one year. ATL06 (Land Ice Height data) data is a derivative of ATL03 data at 20 m intervals in the along-track direction and is considered more suitable for scientific research, with an accuracy of about 3 cm and a precision of about 9 cm on flat areas (Brunt et al., 2021). In this paper, we used ATL06 (version 006) data from April, 2019 to August, 2023 (the first two cycles of ICESat-2 do not form repeat orbits and are therefore not used in this paper) for study. We used the data quality flag to remove potentially problematic ATL06 data points.

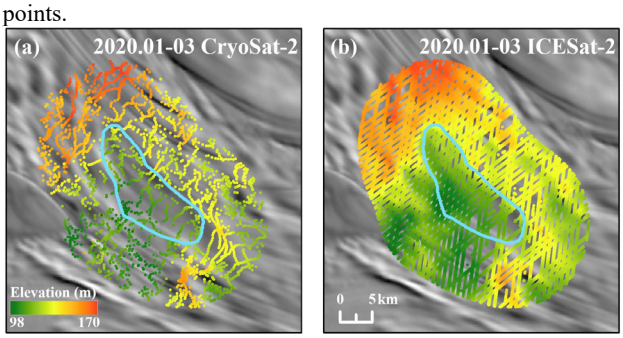

Figure 2. Comparison of two types of altimetry data from January to March 2020. (a) CryoSat-2 data. (b) ICESat-2 data.

2.3 Methods

2.3.1 Differential DEM Model: The CryoSat-2 is a non-repeat altimetry mission, so the CryoSat-2 data are more evenly distributed in the subglacial lake area. Based on these characteristics, we adopted the differential DEM method (Siegfried et al., 2014) to construct the elevation anomaly time series of the ice surface of SLM. The principle of this method is as follows:

First of all, the CryoSat-2 data from January 2011 to June 2011 were used to construct a 100 m resolution base DEM using the Kriging method. After the initial base DEM is generated, the CryoSat-2 points are interpolated to the corresponding position of the DEM, and then the difference between the measured elevation and the interpolated elevation of the DEM is calculated, and then the CryoSat-2 points corresponding to the anomalies are eliminated by using the 3-sig principle. The above process is iterated until there are no more CryoSat-2 points to be eliminated to get the final base DEM. Second, all CryoSat-2 data were then divided into several groups with a three-month time window and a one-month moving step. And then interpolating the points of each group to the corresponding position of the base DEM. After that, we can calculate the elevation anomaly by calculating the difference between the CryoSat-2 measured elevation and the interpolated elevation of the base DEM:

$$dh = \frac{1}{n}\sum_{i=1}^{n} h_m(x,y)_i - h_b(x,y)_i \quad (1)$$

where dh = elevation anomaly
$h_m(x,y)_i$ = CryoSat-2 measured elevation
$h_b(x,y)_i$ = interpolated elevation of the base DEM
n = total number of CryoSat-2 points of each group

In order to eliminate the influence of regional factors such as snow and ice flow on the surface elevation change of the ice sheet, a 10 km buffer is constructed outward from the boundary of SLM (Figure 1). So, we calculate the elevation anomaly in the lake area and the buffer area, respectively, and subtract the value in the lake area from the value in the buffer area to obtain the final elevation anomaly, which eliminates regional influence.

2.3.2 Repeat Track Model: Since ICESat-2 forms repeat tracks on the ground, the elevation anomalies in the subglacial lake region will thus have parabolic features in the along-track direction. However, since this repeat track is not strict, it is necessary to build a repeat track model for slope correction, which is based on the following principle:

For all ICESat-2 points of a single reference ground track (RGT), the data is divided into rectangular strips with 50% overlap in the along-track direction, and the terrain within the strips is fitted according to the repeat track model, which consists of a base terrain term and a time-varying term. On this basis, using the ICESat-2 measured elevations minus the base terrain term, we can get the elevation anomalies of all ICESat-2 points in the rectangular strip after slop correction (Smith et al., 2009).

$$H_r = H(x,y) + \Delta h(t) \quad (2)$$
$$H(x,y) = a_1 + a_2(x-\bar{x}) + a_3(y-\bar{y}) \quad (3)$$
$$\Delta h(t) = a_4(t-t_0) \quad (4)$$
$$dh = H - H(x,y) \quad (5)$$

where H_r = model-fitted terrain
$H(x,y)$ = base terrain term
$\Delta h(t)$ = time-varying term
x, y = the coordinates of each ICESat-2 point
$\bar{x}, \bar{y}$ = average coordinates of all the ICESat-2 points in one rectangular strip
t, t_0 = acquisition time of each ICESat-2 point, the average acquisition time of all data for the first available cycle
a_1, a_2, a_3, a_4 = the coefficients to be solved
H = ICESat-2 measured elevation

And then similarly, according to the method described in 2.3.1, to eliminate the influence of regional factors. If all the tracks are included in the calculation, all the results should be weighted according to the length of the track across the lake, and finally we can get the elevation anomaly that reflects the overall situation of SLM. Because in some areas it is difficult to generate base DEM with high accuracy due to small amounts of data or uneven distribution, this method utilizes the features of the repeat track data for processing and no longer relies on the availability of base DEM. In addition, the accuracy of the data results can be maximized by not introducing external data.

3. Results and Discussions

3.1 Accuracy Evaluation of the Base DEM

The result of the base DEM obtained using CryoSat-2 data from the first half of 2011 is shown in Figure 3a. The lake area of SLM is relatively flat, with an overall elevation of about 100 m and some localized surface uplift in the west and south. The eastern part of SLM has a relatively high elevation, and the eastern boundary of SLM is also the area where the elevation has changed significantly. We interpolated the CryoSat-2 point obtained after several iterations to the corresponding position of the base DEM, calculated the difference between the interpolated elevation and the CryoSat-2 measured elevation, and plotted the histogram of its frequency distribution (Figure 3b and 3c). In general, the base DEM has high accuracy, and the difference conforms to the law of normal distribution, and the mean and standard deviation of the difference are 0.003 and 1.010 m, respectively, indicating the good consistency between these two types of elevations.

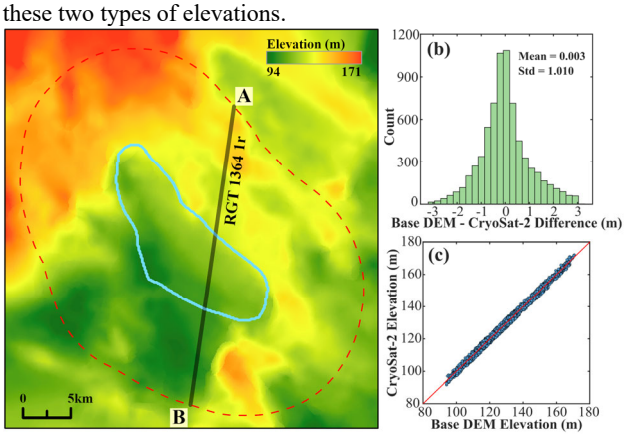

Figure 3. Base Dem and its accuracy result. (a) Base DEM. AB is an ICESat-2 RGT analysed in Figure 5. (b) and (c) Result of the accuracy evaluation of the base DEM.

3.2 Temporal and Spatial Evolution of SLM Based on CryoSat-2

Using the CryoSat-2 data to generate a series of differential DEM images (all compared to the first three months of 2011), the temporal and spatial evolution of the ice surface elevation anomalies of SLM can be clearly portrayed (Figure 4).

From 2011 to the middle of 2012, the overall ice surface elevation within the SLM boundary showed a certain degree of uplift from 3 to 5 m (Figure 4b). And in the second half of 2012 (Figure 4c), a small but aggregated surface subsidence of around -5 to -10 m occurred in the central lake area of SLM, inferring that the drainage event of SLM mainly occurred in this area. From this point until the end of 2014, for nearly two years, SLM was in a significant draining phase (Figure 4d-e). The area with significant elevation anomalies in the west and the area with elevation anomalies that tend to be close to 0 are clearly demarcated and coincide well with the lake boundary. The elevation anomalies in the west can reach about -15 m, while most of them in the east are less than -5 m, indicating that there is a significant difference between the two areas. This suggests that the lake boundary mapped by the previous study is somewhat exaggerated in the eastern area or that the degree of elevation change of the ice sheet surface in the western area is significantly stronger than that in the eastern area during the draining phase. This drainage event was followed by an uplift in the overall ice sheet surface elevation of SLM during 2015-2018 (Figure 4f-g). Among them, in the first half of 2016 (Figure 4f), an area of striped elevation anomalies can be seen to some extent in the western boundary area of SLM. Although the same area also shows a certain degree of striped features on several other images of Figure 4, the elevation anomalies were observed to extend clearly and distinctly into the buffer area of SLM in this time period only. We hypothesized that during this period, the upstream waters were transported into SLM through this location, with a consequent rise in ice sheet surface elevation. Moreover, this strip region happens to be roughly in the drainage path of the previously predicted subglacial water flow path (Siegfried et al., 2023). Beginning in mid-to-late 2018 (Figure 4h-j), another drainage event occurred. However, compared to the first drainage event in 2012, this one was relatively less intense, with maximum elevation anomalies observed around -10 m.

Note that there are some significant clusters of elevation anomalies in the buffer area outside SLM. This is caused by the uneven distribution of CryoSat-2 points and the absence of significant elevation changes in these areas.

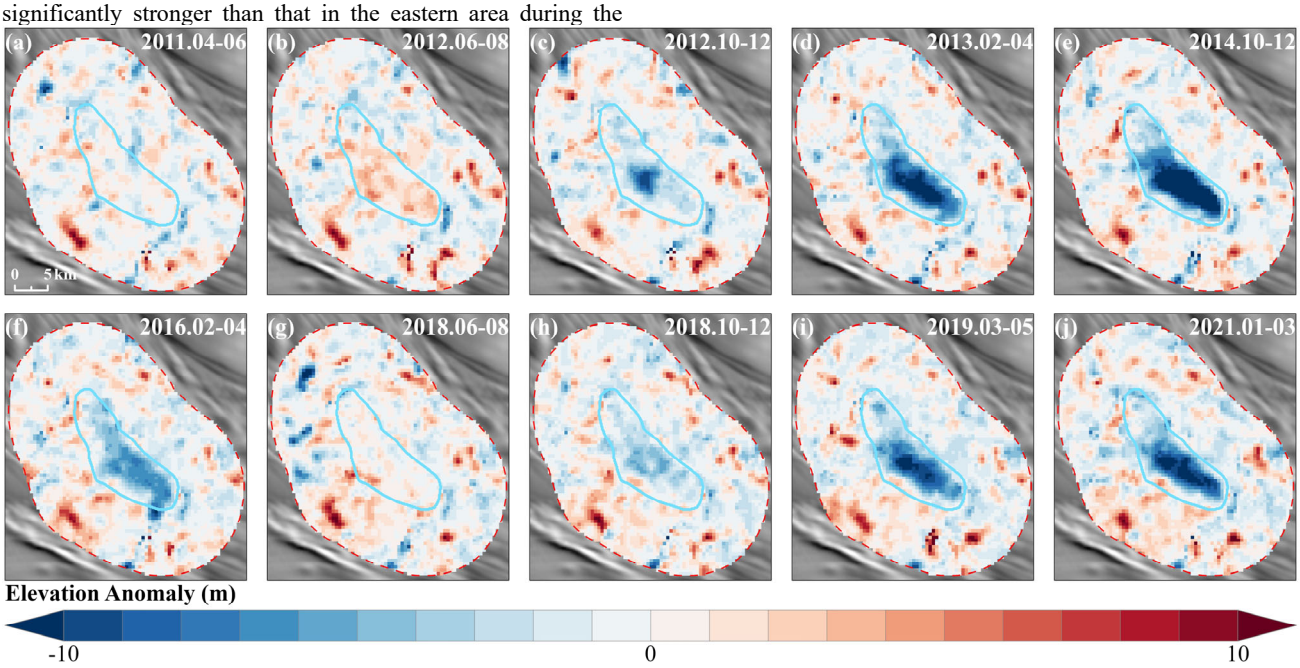

Figure 4. CryoSat-2-derived spatial ice surface elevation anomalies of SLM.

3.3 Temporal and Spatial Evolution of SLM Based on ICESat-2

For ICESat-2 data, the along-track elevation anomalies can be calculated for each RGT based on the repeat track model. Taking ICESat-2 RGT 1364 1r (the right beam of the first pair of beams of RGT 1364) as an example (AB in Figure 3), the elevation and elevation anomaly of each cycle of this RGT are shown in Figure 5 below.

From the elevation curves, there is an obvious area of elevation change in the area where the SLM is located (about 15-20 km along the track, Figure 5a), while the elevation anomaly curves show obvious parabolic characteristics in the same area, and the elevation anomalies are almost zero at other areas except for a few locations (Figure 5b). This is due to the fact that subglacial lake drainage or filling events will lead to changes in the pressure of the overlying ice, and such changes are transmitted differently at different depths and locations, which ultimately results in a large change in elevation in the central part of the lake and a small change in elevation in the surrounding area. In terms of the evolution pattern of elevation anomalies over time, the elevation anomalies of this RGT have an upward trend in the second half of 2019, with a maximum increase of 3 to 4 m. After that, they are in a downward trend until the first half of 2021, with a maximum decrease of 6 to 7 m. From the second half of 2021 until 2023, they are in a significant upward trend, with a maximum increase of about 12 m. In addition, the elevation curves reflect some localized topographic features of SLM, such as the flat topography of the southern boundary area of SLM, which is 10-13 km along the track direction, but the topography begins to drop significantly as it reaches the lake

boundary. However, this phenomenon does not exist in the northern boundary area.

In general, the along-track elevation analysis method of repeated track type altimetry data is widely used in the detection of subglacial lakes. Through the along-track elevation and elevation anomaly curves, the location of subglacial lakes can be clearly determined by their characteristics and the specific values of elevation anomalies, and their changes can be visually reflected.

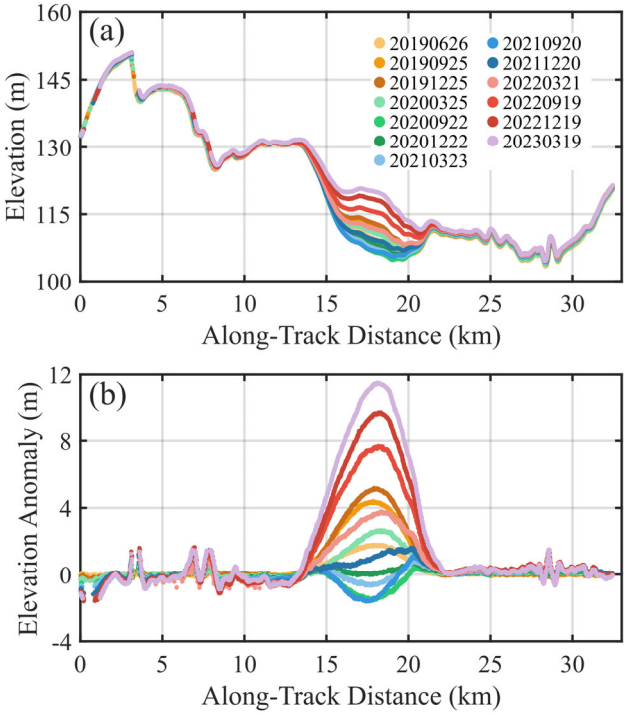

Figure 5. Along-track analysis of ICESat-2 data. (a) Along-track elevation of AB (see Figure 3 for the location of AB), with A as the starting point. (b) Along-track elevation anomaly of AB.

Similar to CryoSat-2, the elevation anomaly results for all RGTs of tICESat-2 data can be plotted as some images of the spatial distribution of elevation anomalies for each cycle (Figure 6). From April 2019 to the end of 2019, the elevations in the western and central parts of SLM show an upward trend of 3-5 m (Figure 6a-b), but the eastern parts show almost no change, inferring that the filling water of SLM in this phase did not reach these areas (Figure 6b). From 2020 until the first half of 2021, SLM was in a drainage period (Figure 6c-f), especially the elevation anomalies at the centre of the lake in the central and western parts of the lake, which were more significant, with the maximum elevation anomaly reaching about -5 m. However, in general, the degree of drainage in this period is not very intense, only limited to the centre of the lake, and there is a slight increase in elevation from the second half of 2020 to the beginning of 2021 (Figure 6d-e). From the end of 2021 to the beginning of 2023, a significant filling event occurred in SLM (Figure 6f-i), and the localized elevation anomalies in SLM could reach about 14 m by the beginning of 2023 (Figure 6i). And relatively more significant elevation anomalies occur in the eastern part of SLM during this period than in the second half of 2019 (Figure 6b), suggesting a higher intensity of water filling during this period. However, starting in 2023 and continuing through midyear (Figure 6i-j), SLM again shows a trend of drainage, with areas of significant elevation anomalies beginning to contract toward the lake and some tracks beginning to have negative elevation anomalies. Note that there is a small area of nulls in the southwest part of SLM at some periods (Figure 6a-b, d, g, and h), an area where an active subglacial lake, LSLM, was detected not long ago (Siegfried and Fricker, 2021), but nulls are present at this lake location due to the outliers culling procedure that we have performed on both the lake area and the buffer area here. Overall, the results of the temporal and spatial evolution analyses of both CryoSat-2 and ICESat-2 indicate that the lake boundary of the SLM is somewhat exaggerated in the east, and the results here of ICESat-2 are in general agreement with the numerical evolution of the single ICESat-2 RGT above.

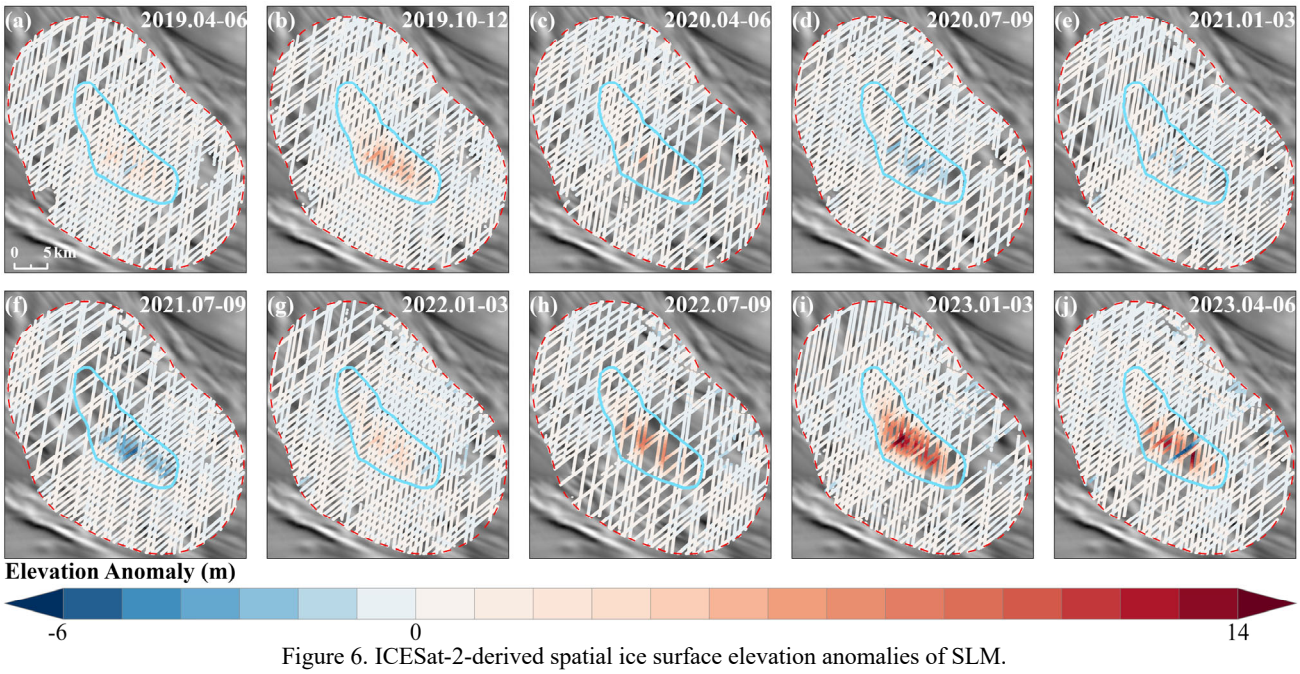

Figure 6. ICESat-2-derived spatial ice surface elevation anomalies of SLM.

3.4 Time Series of Ice Surface Elevation Anomaly

In order to quantitatively portray lake-wide fill-drain events as a whole, we constructed a time series of ice surface elevation anomalies for SLM (Figure 7). Between 2011 and 2023, three significant fill-drain cycle events occurred at SLM.

The first drainage occurred in the second half of 2012 and continued until about 2015, during which time the magnitude of change in the elevation anomaly of SLM reached nearly 8 m or so. However, the time series reveals a slight elevation uptrend in SLM during March to October 2013, and after this period, the elevation downtrend continued. The second drainage occurred in middle 2018, but prior to this time, SLM had been in a steady filling phase since 2015, with a rise in elevation anomaly of about 6 m. However, after 2018, the change in SLM showed a certain oscillatory trend. From April 2019 to the end of 2019, SLM showed an increasing trend in elevation, but then showed a decreasing trend in elevation until a third significant filling event began around August 2021. In total, the second drainage event led to a drop in elevation anomaly around 4 m. The third filling event took only about 1.5 years to start draining again, which is half as long as the second filling event. However, due to the limited time of data acquisition, the duration of the third drainage event and the extent of the decrease in the surface elevation of SLM are not yet known, which will require further observations in the future. In addition, the surface elevation of SLM did not return to the elevation before the first drainage event after the last two filling events, presumably because the first drainage resulted in mass loss under the ice sheet, thus making it difficult to return to the initial elevation state during the later filling. Combining the time series results of CryoSat-2 and ICESat-2, the two results match well during the nearly two-year mission overlap time in 2019-2021, which illustrates the effectiveness of the two different altimetry data processing methods and further supports the existence of a certain degree of oscillation of the surface elevation of SLM during the second drainage event.

It should be noted that the results of time series reflect an average trend, not a specific region of SLM, and thus the specific values of elevation anomalies differ from those analyzed in the previous analysis of the temporal and spatial evolution patterns, but the overall temporal pattern of the SLM evolution remains consistent.

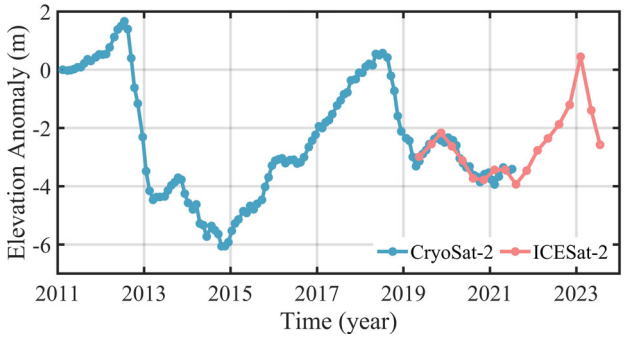

Figure 7. Ice surface elevation anomaly time series of SLM.

4. Conclusions

In this paper, CryoSat-2 satellite radar altimetry data and ICESat-2 satellite laser altimetry data are jointly used to monitor the fill-drain events of the active subglacial lake SLM located in West Antarctica during the period 2011-2023. In this case, a differential DEM model based on the generation of a base DEM was used for the CryoSat-2, while a repeat track model that does not depend on the introduction of external data was used for the ICESat-2. On this basis, this study plotted the spatial elevation anomaly images under the two types of altimetry data and finally constructed a complete ice surface elevation anomaly time series, revealing the spatial evolution pattern and numerical characteristics of the activity of SLM.

The results show that three fill-drain events occurred in SLM during the study period. In terms of spatial evolution, both the spatial elevation anomaly images of CryoSat-2 and ICESat-2 found that the central and western parts of SLM were the areas of more intense subglacial lake activity, thus the eastern area was presumed to have an exaggerated lake area. In terms of numerical characteristics, the first drainage event was the most intense, with changes in elevation anomalies reaching about 8 m, nearly twice as large as those of the second drainage event, and likely resulting in some mass loss under the ice. Finally, methodologically, the results of the two methods are highly compatible during the mission overlap period, verifying the feasibility of the methods and the accuracy of the results. This study focuses more on the remote sensing observation of subglacial lake activities, and in the future, we can consider mathematical modelling combined with RES data to analyze the formation and development of subglacial lakes in terms of physical mechanisms and further analyze the potential impacts on the mass balance of the Antarctic coastal region.

Acknowledgements

This research was supported by the Shanghai Science and Technology Innovation Action Plan-International Science and Technology Cooperation Program (No. 23230712200), the National Natural Science Foundation of China (No. 42394131, 42276249, and 42111530185), and the Fundamental Research Funds for the Central Universities.

References

Brunt, K.M., Smith, B.E., Sutterley, T.C., Kurtz, N.T., Neumann, T.A., 2021. Comparisons of Satellite and Airborne Altimetry With Ground-Based Data From the Interior of the Antarctic Ice Sheet. *Geophysical Research Letters* 48, e2020GL090572. doi.org/10.1029/2020GL090572.

Carter, S.P., Fricker, H.A., Siegfried, M.R., 2017. Antarctic subglacial lakes drain through sediment-floored canals: theory and model testing on real and idealized domains. *The Cryosphere* 11, 381–405. doi.org/10.5194/tc-11-381-2017.

Carter, S.P., Fricker, H.A., Siegfried, M.R., 2013. Evidence of rapid subglacial water piracy under Whillans Ice Stream, West Antarctica. *Journal of Glaciology* 59, 1147–1162. doi.org/10.3189/2013JoG13J085.

Christianson, K., Jacobel, R.W., Horgan, H.J., Anandakrishnan, S., Alley, R.B., 2012. Subglacial Lake Whillans—Ice-penetrating radar and GPS observations of a shallow active reservoir beneath a West Antarctic ice stream. *Earth and Planetary Science Letters* 331, 237–245. doi.org/10.1016/j.epsl.2012.03.013.

Fan, Y., Hao, W., Zhang, B., Ma, C., Gao, S., Shen, X., Li, F., 2022. Monitoring the Hydrological Activities of Antarctic Subglacial Lakes Using CryoSat-2 and ICESat-2 Altimetry Data. *Remote Sensing* 14. doi.org/10.3390/rs14040898.

Flament, T., Berthier, E., Rémy, F., 2014. Cascading water underneath Wilkes Land, East Antarctic ice sheet, observed using altimetry and digital elevation models. *The Cryosphere* 8, 673–687. doi.org/10.5194/tc-8-673-2014.

Fricker, H.A., Carter, S.P., Bell, R.E., Scambos, T., 2014. Active lakes of Recovery Ice Stream, East Antarctica: a bedrock-controlled subglacial hydrological system. *Journal of Glaciology* 60, 1015–1030. doi.org/10.3189/2014JoG14J063.

Fricker, H.A., Scambos, T., Bindschadler, R., Padman, L., 2007. An Active Subglacial Water System in West Antarctica Mapped from Space. *Science* 315, 1544–1548. doi.org/10.1126/science.1136897.

Gardner, A.S., Moholdt, G., Scambos, T., Fahnstock, M., Ligtenberg, S., van den Broeke, M., Nilsson, J., 2018. Increased West Antarctic and unchanged East Antarctic ice discharge over the last 7 years. *The Cryosphere* 12, 521–547. doi.org/10.5194/tc-12-521-2018.

Horgan, H.J., Anandakrishnan, S., Jacobel, R.W., Christianson, K., Alley, R.B., Heeszel, D.S., Picotti, S., Walter, J.I., 2012. Subglacial Lake Whillans—Seismic observations of a shallow active reservoir beneath a West Antarctic ice stream. *Earth and Planetary Science Letters* 331, 201–209. doi.org/10.1016/j.epsl.2012.02.023.

Kim, B.-H., Lee, C.-K., Seo, K.-W., Lee, W.S., Scambos, T., 2016. Active subglacial lakes and channelized water flow beneath the Kamb Ice Stream. *The Cryosphere* 10, 2971–2980. doi.org/10.5194/tc-10-2971-2016.

Livingstone, S.J., Li, Y., Rutishauser, A., Sanderson, R.J., Winter, K., Mikucki, J.A., Björnsson, H., Bowling, J.S., Chu, W., Dow, C.F., Fricker, H.A., McMillan, M., Ng, F.S.L., Ross, N., Siegert, M.J., Siegfried, M., Sole, A.J., 2022. Subglacial lakes and their changing role in a warming climate. *Nature Reviews Earth & Environment* 3, 106–124. doi.org/10.1038/s43017-021-00246-9.

Malczyk, G., Gourmelen, N., Goldberg, D., Wuite, J., Nagler, T., 2020. Repeat Subglacial Lake Drainage and Filling Beneath Thwaites Glacier. *Geophysical Research Letters* 47, e2020GL089658. doi.org/10.1029/2020GL089658.

Markus, T., Neumann, T., Martino, A., Abdalati, W., Brunt, K., Csatho, B., Farrell, S., Fricker, H., Gardner, A., Harding, D., Jasinski, M., Kwok, R., Magruder, L., Lubin, D., Luthcke, S., Morison, J., Nelson, R., Neuenschwander, A., Palm, S., Popescu, S., Shum, C., Schutz, B.E., Smith, B., Yang, Y., Zwally, J., 2017. The Ice, Cloud, and land Elevation Satellite-2 (ICESat-2): Science requirements, concept, and implementation. *Remote Sensing of Environment* 190, 260–273. doi.org/10.1016/j.rse.2016.12.029.

McMillan, M., Corr, H., Shepherd, A., Ridout, A., Laxon, S., Cullen, R., 2013. Three-dimensional mapping by CryoSat-2 of subglacial lake volume changes. *Geophysical Research Letters* 40, 4321–4327. doi.org/10.1002/grl.50689.

Miles, B.W.J., Stokes, C.R., Jamieson, S.S.R., 2018. Velocity increases at Cook Glacier, East Antarctica, linked to ice shelf loss and a subglacial flood event. *The Cryosphere* 12, 3123–3136. doi.org/10.5194/tc-12-3123-2018.

Oswald, G.K.A., Robin, G.D.Q., 1973. Lakes Beneath the Antarctic Ice Sheet. *Nature* 245, 251–254. doi.org/10.1038/245251a0.

Priscu, J.C., Kalin, J., Winans, J., Campbell, T., Siegfried, M.R., Skidmore, M., Dore, J.E., Leventer, A., Harwood, D.M., Duling, D., 2021. Scientific access into Mercer Subglacial Lake: scientific objectives, drilling operations and initial observations. *Annals of Glaciology* 62, 340–352. doi.org/10.1017/aog.2021.10.

Scambos, T.A., Berthier, E., Shuman, C.A., 2011. The triggering of subglacial lake drainage during rapid glacier drawdown: Crane Glacier, Antarctic Peninsula. *Annals of Glaciology* 52, 74–82. doi.org/10.3189/172756411799096204.

Scambos, T.A., Haran, T.M., Fahnestock, M.A., Painter, T.H., Bohlander, J., 2007. MODIS-based Mosaic of Antarctica (MOA) data sets: Continent-wide surface morphology and snow grain size. *Remote Sensing of Environment, Remote Sensing of the Cryosphere Special Issue* 111, 242–257. doi.org/10.1016/j.rse.2006.12.020.

Siegert, M.J., Ross, N., Corr, H., Smith, B., Jordan, T., Bingham, R.G., Ferraccioli, F., Rippin, D.M., Le Brocq, A., 2014. Boundary conditions of an active West Antarctic subglacial lake: implications for storage of water beneath the ice sheet. *The Cryosphere* 8, 15–24. doi.org/10.5194/tc-8-15-2014.

Siegfried, M.R., Fricker, H.A., 2021. Illuminating Active Subglacial Lake Processes With ICESat-2 Laser Altimetry. *Geophysical Research Letters* 48, e2020GL091089. doi.org/10.1029/2020GL091089.

Siegfried, M.R., Fricker, H.A., 2018. Thirteen years of subglacial lake activity in Antarctica from multi-mission satellite altimetry. *Annals of Glaciology* 59, 42–55. doi.org/10.1017/aog.2017.36.

Siegfried, M.R., Fricker, H.A., Roberts, M., Scambos, T.A., Tulaczyk, S., 2014. A decade of West Antarctic subglacial lake interactions from combined ICESat and CryoSat-2 altimetry. *Geophysical Research Letters* 41, 891–898. doi.org/10.1002/2013GL058616.

Siegfried, M.R., Venturelli, R.A., Patterson, M.O., Arnuk, W., Campbell, T.D., Gustafson, C.D., Michaud, A.B., Galton-Fenzi, B.K., Hausner, M.B., Holzschuh, S.N., Huber, B., Mankoff, K.D., Schroeder, D.M., Summers, P.T., Tyler, S., Carter, S.P., Fricker, H.A., Harwood, D.M., Leventer, A., Rosenheim, B.E., Skidmore, M.L., Priscu, J.C., the SALSA Science Team, 2023. The life and death of a subglacial lake in West Antarctica. *Geology* 51, 434–438. doi.org/10.1130/G50995.1.

Smith, B.E., Fricker, H.A., Joughin, I.R., Tulaczyk, S., 2009. An inventory of active subglacial lakes in Antarctica detected by ICESat (2003–2008). *Journal of Glaciology* 55, 573–595. doi.org/10.3189/002214309789470879.

Smith, B.E., Gourmelen, N., Huth, A., Joughin, I., 2017. Connected subglacial lake drainage beneath Thwaites Glacier, West Antarctica. *The Cryosphere* 11, 451–467. doi.org/10.5194/tc-11-451-2017.

Stearns, L.A., Smith, B.E., Hamilton, G.S., 2008. Increased flow speed on a large East Antarctic outlet glacier caused by

subglacial floods. *Nature Geoscience* 1, 827–831. doi.org/10.1038/ngeo356.

Tulaczyk, S., Mikucki, J.A., Siegfried, M.R., Priscu, J.C., Barcheck, C.G., Beem, L.H., Behar, A., Burnett, J., Christner, B.C., Fisher, A.T., 2014. WISSARD at Subglacial Lake Whillans, West Antarctica: scientific operations and initial observations. *Annals of Glaciology* 55, 51–58. doi.org/10.3189/2014AoG65A009.

Wang, F., Bamber, J.L., Cheng, X., 2015. Accuracy and Performance of CryoSat-2 SARIn Mode Data Over Antarctica. *IEEE Geoscience and Remote Sensing Letters* 12, 1516–1520. doi.org/10.1109/LGRS.2015.2411434.

Wingham, D.J., Siegert, M.J., Shepherd, A., Muir, A.S., 2006. Rapid discharge connects Antarctic subglacial lakes. *Nature* 440, 1033–1036. doi.org/10.1038/nature04660.